ELSEVIER

Journal of Non-Crystalline Solids 299–302 (2002) 1100–1104

JOURNAL OF NON-CRYSTALLINE SOLIDS

www.elsevier.com/locate/jnoncrysol

Formation of CdS nanocrystals in SiO_2 by ion implantation

U.V. Desnica [a,*], I.D. Desnica-Frankovic [a], O. Gamulin [b], C.W. White [c], E. Sonder [c], R.A. Zuhr [c]

[a] *Department of Physics, R. Boskovic Institute, Bijenicka 54, HR-10000 Zagreb, Croatia*
[b] *School of Medicine, Zagreb University, Salata 3, HR-10000 Zagreb, Croatia*
[c] *Oak Ridge National Laboratory, P.O. Box 2008, Oak Ridge, TN 37831, USA*

Abstract

We present a systematic study of the influence of ion dose and post-implantation annealing on the synthesis and growth of CdS nanocrystals in a SiO_2 matrix. Nanocrystals were obtained after implantation of monoenergetic Cd and S ions and subsequent annealing in a very wide range of annealing temperatures, T_a. The average size, as determined from the blue shift of band gap E_g, varied from 3.5–4.5 to 10 nm, depending on implantation and annealing parameters. For the highest dose, 10^{17} ions/cm^2, the synthesis of CdS phase starts already during implantation. For T_a above 700 °C, large nanocrystals (9–10 nm) prevail for all doses. High energy optical transitions, identified as the E_{1A} and E_{1B} transitions of hexagonal CdS, were also observed after annealings at higher temperature.

PACS: 81.05.y; 78.40.F; 61.72.V; 78.20.C

1. Introduction

Systems of small dimensions (nanocrystals or quantum dots), exhibit considerably different optical and electronic properties from bulk semiconductors due to the quantum confinement of free carriers. Semiconductor–glass composites posses substantial third-order optical non-linear coefficients at room temperature [1], and as such have a potential for interesting applications in optical devices such as waveguides, high-speed optical switches, or bistable resonators.

Ion implantation, as a novel method for the production of encapsulated quantum dots in an insulating matrix [2–7], offers more freedom from thermodynamical limitations, extreme chemical purity, exceptional versatility/flexibility in the choice of active components and the underlying matrix, and compatibility with planar technology. Implantation maximizes external control over the process of nanocrystal synthesis, enabling a very wide range of concentrations (possibility for a much denser packing of nanocrystals), desired thickness of the implanted layer, desirable radial and axial doping profiles, and excellent control and reproducibility once the optimal implantation parameters are determined. Up to now, the feasibility of forming nanocrystals by this method has been demonstrated for semiconductors from

* Corresponding author. Tel.: +385-1 4561 173; fax: +385-1 4680 114.
E-mail address: desnica@rudjer.irb.hr (U.V. Desnica).

0022-3093/02/$ - see front matter
PII: S0022-3093(02)00941-9

group IV, group III–V and most of the group II–VI.

In this work we present a systematic study of the influence of ion dose and post-implantation annealing in a very wide range of annealing temperatures on the synthesis and growth of CdS nanocrystals in a SiO_2 matrix.

2. Experimental details

CdS nanocrystals in the SiO_2 (amorphous) substrate were created by sequential implantation of monoenergetic Cd and S ions and subsequent thermal processing, which caused the diffusion of implanted ions and their synthesis into a new phase, CdS. The 2 cm diameter fused silica (Corning 7940) substrates, 1 mm thick, were implanted with equal doses of 320 keV Cd and 115 keV S ions. Three different ion doses were applied: $D1 = 2.5 \times 10^{16}$, $D2 = 5 \times 10^{16}$, and $D3 = 1 \times 10^{17}$ ions/cm^2. The resulting peak volume concentrations were 2.0×10^{21}/cm^3, 3.4×10^{21}/cm^3 and 6.3×10^{21}/cm^3 of both Cd and S atoms, as determined by Rutherford back scattering. The chosen implant energies resulted in very similar depth profiles (maximum concentrations at ~130 nm and total depths about ~260 nm). After implantation each wafer was cut into six pieces; five of these were annealed for 1 h at five different temperatures, and the sixth was kept unannealed to form a reference set (RT annealing). The annealing temperatures, T_a, were 300, 500, 700, 800 and 900 °C. Another reference set consisted of unimplanted SiO_2 samples, which were heated to the same annealing temperatures as the implanted samples. Optical characterization was undertaken with a Unicam UV/VIS 4 spectrometer, in the 1.5–6.5 eV range.

3. Results

The ion dose dependence of the absorption edge (band gap, E_g), after annealing at the same temperature $T_a = 700$ °C, is presented in Fig. 1. The SiO_2 substrate is highly transparent in the whole measured frequency range (absorbance, A, smaller

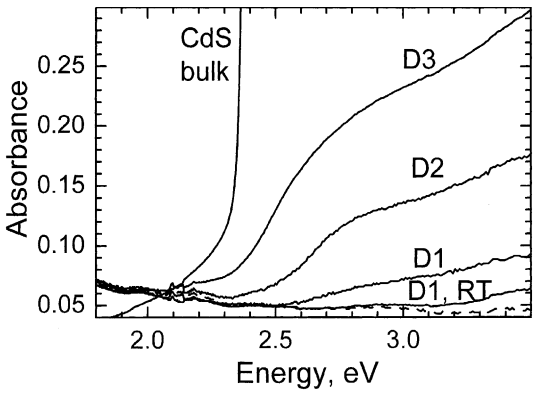

Fig. 1. Representative optical absorption spectra of CdS–SiO_2 composites showing effects of various ion doses at selected annealing temperature (700 °C). $D1$, $D2$ and $D3$ refer to the implanted doses of 2.5×10^{16}, 5×10^{16} and 1×10^{17} ions/cm^2 of Cd and S atoms, respectively. $D1$, RT denoted absorption spectrum for implanted (dose $D1$) but unannealed sample, while the dashed line shows the absorption spectrum of the SiO_2 substrate.

than 0.07). Hence, the strong increase of optical density for energies around and above 2.5 eV is considered as a quantitative measure of the formation of the CdS phase in the SiO_2 matrix. The E_g shifts to higher energy (blue shift) as the ion dose decreases. The presence of the implanted foreign atoms, particularly Cd, also somewhat increases the absorption at higher energy but considerably less than the presence of the CdS phase. This contribution certainly decreases significantly with annealing, when most of the free atoms become consumed into CdS crystallites. To study the changes of the absorption edge with the nanocrystal size more quantitatively the numerical first derivative of the absorbance was used (Figs. 2 and 3(b)), since in this representation the shift of the peak towards higher energies is better observable. The blue shift of the maximum of the first derivative of the absorbance corresponds to the blue shift of E_g [8,9]. The influence of the ion dose on the position of the maximum of the first derivative (for a given T_a) is shown in Fig. 2(a), while Fig. 2(b) demonstrates the influence of T_a (for a given ion dose). It is interesting that, beside the dominant peak, several additional local maxima in the first derivative are distinguishable. These additional maxima group at specific energies.

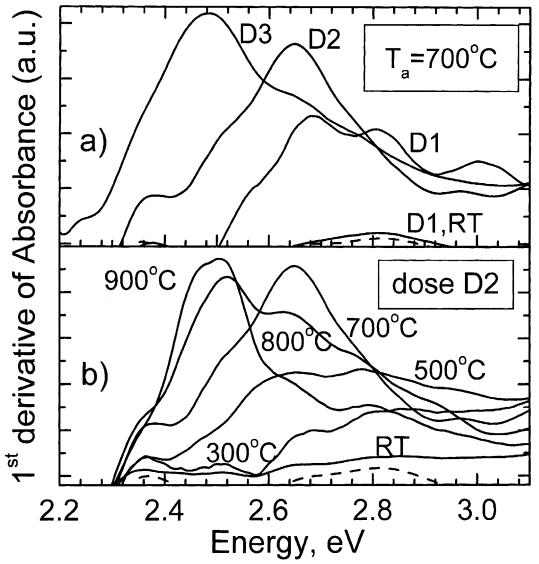

Fig. 2. The influence of the (a) ion dose and (b) annealing temperature on the numerical first derivatives of the absorption spectra. Doses and annealing temperatures are indicated.

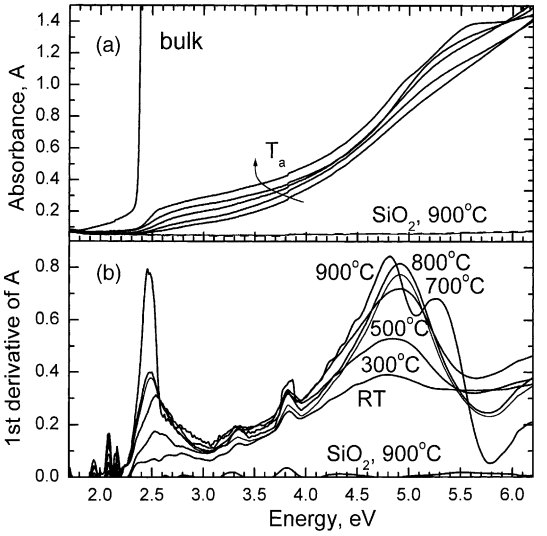

Fig. 3. (a) Optical absorption spectra, and (b) their first derivatives, of a series of samples implanted with an ion dose of 10^{17}/cm^2 Cd and S atoms and annealed at different temperatures. The features at 3.3 and 3.8 eV are instrumental artifacts. The absorbance of unannealed SiO_2 and SiO_2 annealed to 900 °C (SiO_2, 900) were indistinguishable.

Analogous results were obtained for other doses and other values of T_a.

Absorption spectra in the 1.5–6.5 eV range for samples implanted with dose $D3$ and annealed at different T_a are presented in Fig. 3. The absorption features in the extended UV frequency region proved useful for substantiating the identity of the new crystalline phase in the amorphous SiO_2. These features are again more readily observable in the first derivative spectrum (Fig. 3(b)), which shows well-defined maxima at 4.8 and 5.4 eV. For lower T_a the first derivative exhibits only one maximum at about 4.9 eV. For the lowest dose $D1$ (not shown) the substantial absorption around 2.5 eV begins only after annealings above 500 °C, but it starts earlier for higher doses. For dose $D3$ it is considerable even before annealing.

4. Discussion

Quantum size effects arise in the semiconductor–glass composite when small, isolated semiconductor crystals are formed in an insulating matrix. Quantum confinement in our CdS–glass composites was confirmed by the energy shifts in the optical absorbance spectra. By using a model based on the effective-mass approximation and including a Coulombic interaction term proposed by Brus [10], one can relate the blue shift, ΔE_g, to the average size (diameter) of nanocrystals, d [2,10]:

$$\Delta E_g = (2h\pi^2/\mu d^2) - (3.6e^2/\varepsilon d), \quad (1)$$

where h, μ, e, and ε are Planck's constant, the exciton reduced mass in CdS, the electron charge, and the dielectric constant of CdS, respectively. Although this equation gives a systematic error in some cases [8], it seems that it can be reasonably well applied to CdS nanocrystals in SiO_2. For three samples, for which the average sizes were determined (after $T_a = 1000$ °C) from the absorption shift and by TEM, the agreement between both methods as well as with d using the Eq. (1) was satisfactory [4]. Using Eq. (1) and the experimental band gap shifts we have estimated the average diameter of the nanocrystals for each particular combination of ion dose and annealing temperature. A summary of the results is presented

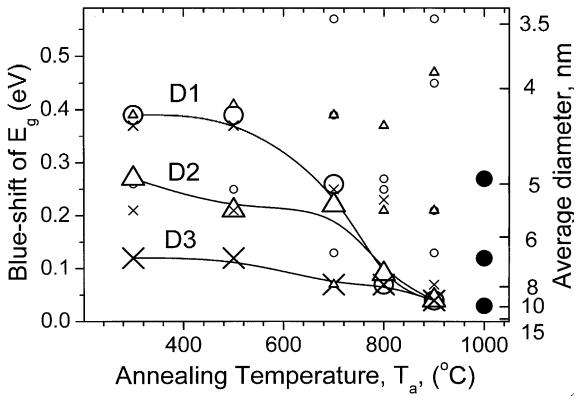

Fig. 4. Band gap shift for CdS nanocrystals as a function of ion dose and annealing temperature derived from the position of the first derivative maxima. Additional local minima are also shown with smaller symbols. Right-side axis shows the average particle diameter calculated from Eq. (1). Full symbols show average particle diameter reported in Ref. [4], as determined by TEM, obtained after multiple-energy implantations. For all samples (including those from Ref. [4]) the annealing times were 1 h. Uncertainty of the band gap shift was ±10%.

in Fig. 4. The blue shift is systematically larger for lower ion doses and for lower annealing temperatures. The average size of the nanocrystals (Fig. 4, right axis) ranges from 3.5–4.5 nm to about 10 nm. The dose and T_a dependence is considerable only for T_a up to 700 °C. However, at these lower values of T_a not all the Cd and S atoms are synthesized yet (note the strong increase with T_a of the CdS-related signal at around 2.5 eV; Fig. 3).

Therefore, annealing temperatures above >700 °C are needed to obtain a large CdS fraction, but in these cases also the average crystallite size becomes large (~10 nm) and similar for all three doses (Fig. 4). This is probably a consequence of very high peak volume concentrations in single-energy implantation. Quite different results were obtained for analogous CdS/SiO_2 samples, reported in [4] (full circles in Fig. 4), which were implanted with similar doses (1×10^{16}, 2.8×10^{16}, and 7.5×10^{16} ions/cm^2), but with multiple ion energies and, therefore, flat depth distributions. Although in [4] the authors did not study the size dependence on T_a, it is obvious that even at T_a as high as 1000 °C, the average size still remains strongly dose dependent. Hence, multiple-energy implantation seems substantial to obtain better control not only of the size distribution [2,4], but also of the particle average size, particularly at higher annealing temperatures.

For dose $D3$ some synthesis of the CdS phase occurs already during implantation (Fig. 3), while the annealing at higher T_a just increases the fraction and particularly the size of the CdS nanocrystals. The appearance of additional local maxima in first derivative is not completely understood at present. It might suggest that CdS nanocrystals do not have a continuous size distribution but several preferential sizes. This puzzling result requires further investigation. The more than doubled absorption, when going from $D1$ to $D2$ and from $D2$ to $D3$, at any particular energy (Fig. 1), suggests that there is no loss of CdS or its constituents due to annealing at higher T_a. Such a loss, due to evaporation, oxidation or formation of a third phase, was observed for some other II–VI compounds formed by implantation in glass, in particular for ZnS [4] and ZnTe [7], as well as for CdTe obtained by RF sputtering [8].

We have identified two high-energy absorption features (Fig. 3) as the E_{1A} and E_{1B} transitions of hexagonal CdS, associated with the 3D M_1 critical point. The absorption coefficient in this energy range is very high (close to 10^6 cm^{-1}) [11], and hence it is generally very difficult to distinguish details in the absorbance of bulk CdS samples. Here it was possible to detect these transitions owing to the low absorption of the thin composite implanted layer. Their maxima in the $D3$ sample correspond precisely to the values obtained by spectroscopic ellipsometry measurement [11], for bulk material (4.8 and 5.5 eV). They were also observed in the $D2$ and $D1$ samples after $T_a =$ 900 °C annealings at exactly the same energy positions. Hence, the nanocrystal size might influence less the position of E_{1A} and E_{1B} and more the broadening of these features, resulting in an overlap. The positions of the maximum in the first derivative spectra, observed for lower T_a (Fig. 3b) for all doses, excludes some alternative explanations, such as the formation of cubic CdS or preferential orientation of nanocrystals. In both of these cases the peak would be at about 5.5 eV at RT.

5. Conclusions

CdS nanocrystals were formed in amorphous SiO_2 by sequential implantation of equal doses of monoenergetic Cd and S ions and subsequent annealing. The average size of the nanocrystals ranged from 3.5–4.5 to 10 nm depending on ion dose and annealing temperature. For the highest ion dose (1×10^{17} ions/cm^2), the formation of the CdS phase apparently starts already during implantation, and a T_a as low as 300 °C is sufficient to produce crystallites with an average diameter of 7 nm. For lower doses the growth of large nanocrystals starts above 700 °C, so that at $T_a = 900$ °C similarly large nanocrystals (about 10 nm) prevail for all doses. These findings differ considerably from the situation when CdS nanocrystals were obtained with comparable ion doses but with multiple-energy implantations, in which case a considerable difference in average size remained even at $T_a = 1000$ °C. The high-energy transitions, identified as E_{1A} and E_{1B}, were also observed for higher annealing temperatures.

Acknowledgements

This research was supported by the Ministry of Science and Technology of Croatia. A portion of this research was performed at Oak Ridge National Laboratory, managed by UT-Battelle, LLC, for the US Department of Energy under contract DE-AC05-00OR22725.

References

[1] R.K. Jain, R.C. Lind, J. Opt. Soc. Am. 73 (1983) 647.
[2] C.W. White, A. Meldrum, J.D. Budai, S.P. Withrow, E. Sonder, R.A. Zuhr, D.M. Hembree Jr., M. Wu, D.O. Henderson, Nucl. Instrum. Meth. Phys. B 148 (1999) 991.
[3] J.D. Budai, C.W. White, S.P. Withrow, M.F. Chisholm, J. Zhu, R.A. Zuhr, Nature 390 (1997) 384.
[4] A. Meldrum, E. Sonder, R.A. Zuhr, I.M. Anderson, J.D. Budai, C.W. White, L.A. Boatner, J. Mater. Res. 14 (1999) 4489.
[5] A. Meldrum, L.A. Boatner, C.W. White, Nucl. Instr. Meth. Phys. B 178 (2001) 7.
[6] U.V. Desnica, O. Gamulin, A. Tonejc, M. Ivanda, C.W. White, E. Sonder, R.A. Zuhr, Mater. Sci. Eng. C, 15 (2001) 105.
[7] H. Karl, I. Grosshans, W. Attenberger, M. Smchmid, B. Stritzger, Nucl. Instrum. Meth. Phys. B 178 (2001) 126.
[8] B.G. Potter Jr., J.H. Simmons, J. Appl. Phys. 68 (1990) 1218.
[9] M. Sotelo-Lerma, M.A. Quevedo-Lopez, R.A. Orozco-Teranm, R. Ramirez-Bon, F.J. Espinoza-Beltran, J. Phys. Chem. Solids 59 (1988) 145.
[10] L.E. Brus, J. Chem. Phys. 80 (1984) 4403.
[11] S. Ninomiya, S. Adachi, J. Appl. Phys. 78 (1995) 1183.